LAWRENCE
LIVERMORE
NATIONAL
LABORATORY

LLNL-JRNL-408318

Corrugation of Phase-Separated Lipid Bilayers Supported by Nanoporous Silica Xerogel Surfaces

E. I. Goksu , B. A. Nellis, W-C. Lin, J. H. Satcher Jr., J. T. Groves, S. H. Risbud, M. L. Longo

October 31, 2008

Langmuir

Disclaimer

Corrugation of Phase-Separated Lipid Bilayers Supported by Nanoporous Silica Xerogel Surfaces

Emel I. Goksu [†], Barbara A. Nellis[†,‡], Wan-Chen Lin[§], Joe Satcher[‡], Jay T. Groves[§], Subhash H. Risbud,[†] and Marjorie L. Longo*[,†]

[†]Department of Chemical Engineering & Materials Science, University of California, Davis, CA 95616

[‡]Chemistry, Materials, Earth and Life Sciences Directorate, Lawrence Livermore National Laboratory, 7000 East Avenue, Livermore, CA 94550

[§]Department of Chemistry, University of California, Berkeley, CA 94720

* corresponding author email: mllongo@ucdavis.edu

Running Head: Domain Formation on Xerogels

Abstract

Lipid bilayers supported by substrates with nanometer-scale surface corrugations holds interest in understanding both nanoparticle-membrane interactions and the challenges of constructing models of cell membranes on surfaces with desirable properties, e.g. porosity. Here, we successfully form a two-phase (gel-fluid) lipid bilayer supported by nanoporous silica xerogel. Surface topology, diffusion, and lipid density in comparison to mica-supported lipid bilayers were characterized by AFM, FRAP, FCS, and quantitative fluorescence microscopy, respectively. We found that the two-phase lipid bilayer follows the xerogel surface contours. The corrugation imparted on the lipid bilayer results in a lipid density that is twice that on a flat mica surface. In direct agreement with the doubling of actual bilayer area in a projected area, we

find that the lateral diffusion coefficient (D) of lipids on xerogel (~1.7 $\mu m^2/s$) is predictably lower than on mica (~4.1 $\mu m^2/s$) by both FRAP and FCS techniques. Furthermore, the gel-phase domains on xerogel compared to mica were larger and less numerous. Overall, our results suggest the presence of a relatively defect-free continuous two-phase bilayer that penetrates approximately midway into the first layer of ~50 nm xerogel beads.

Introduction

Two-dimensional assemblies of phospholipid bilayer membranes supported on solid substrates are referred to as supported lipid bilayers and have been explored as biomimetic analogues of cell membranes. Due to their inherent materials properties; different supports for lipid bilayers offer certain advantages while suffering from several disadvantages. Silicon oxide has been recognized as one of the most feasible surfaces as a support. Lipid bilayer membranes on silicon oxide are supported by a thin lubricating layer of water approximately 1 to 2 nm in thickness.[1,2] However, it has been shown by previous studies on protein insertions that the water layer does not provide enough separation between the membranes and the substrates resulting in non-physiological interactions of transmembrane proteins with the supports.[3] In addition, one of the leaflets of the bilayer is not accessible in these systems. Hence, supporting the lipid bilayers with appropriate substrate to form a better biomimetic system is still challenging.

Recently, there has been a growing interest in porous substrates as a means to overcome these issues. Previous research on porous alumina[4-6] and silica[7-9] surfaces showed that lipid bilayer formation can be accomplished on porous surfaces. Furthermore, lateral mobility of the lipids within the bilayer structure was confirmed on silica xerogel and aerogel surfaces prepared via the sol-gel process.[8, 9] The diffusion coefficient of the lipids were observed to be decreasing as the

porosity of the substrate increased. This was attributed to the sensitivity of the lipid mobility to the local defects and the landscape of the underlying surface. Those findings are promising in terms of potential future studies on the structure and functionality of the lipid bilayers supported by porous silica substrates.

Various studies directed at the mammalian cell plasma membrane have provided evidence for the existence of heterogeneities in the submicron range which are integrally involved with several cell functions such as cell signaling[10], protein sorting[11] and trafficking of proteins and lipids[12]. Therefore, construction of a model membrane with the basic elements associated with membrane heterogeneity provides the most flexible platform for model membrane studies. Although the formation of the lipid bilayers on corrugated surfaces was reported for one phase lipid bilayers, to our knowledge, the formation of lipid domains has not been considered extensively in the literature yet.

In this study, two-phase supported lipid bilayers containing 1,2-Dioleoyl-Glycero-3-Phosphocholine (DOPC) and 1,2-Distearoyl-Glycero-3-Phosphocholine (DSPC) with a mole ratio of 2:1 were prepared on porous silica xerogel surfaces and domain formation was observed. The presence of the domains not only constituted a better biomimetic system but also allowed us to determine the surface coverage. The surface topologies of both the xerogel surface and the lipid bilayer were investigated by Atomic Force Microscopy (AFM) and compared to mica supported lipid bilayers. The lateral diffusion coefficients of the lipids on silica xerogels and mica were compared by both FRAP and FCS techniques. The basic reason underlying the differences in the diffusion coefficients was examined. The domain sizes and density on xerogel vs. mica substrates were compared using fluorescence microscopy.

Materials and Methods

Synthesis of the silica xerogel thin film supports: A one-step base catalyzed sol-gel synthesis procedure was used to form the silica gel. 8.6 g of tetramethyloxysilane (TMOS, Acros Organics, Morris Plains, NJ) was mixed with 15.1 g of methanol (ACS Reagent, Sigma-Aldrich, Milwaukee, WI) for 15 min. In a separate beaker, 3.05 g of water, 15.1 g of methanol, and 100 μL of a 6 M aqueous ammonium hydroxide (Sigma-Aldrich, Milwaukee, WI) solution were mixed for 15 min. Two mixtures were then combined such that the molar ratio for TMOS: H_20: NH_4OH: MeOH was 1:0.33:20:0.06. This resulted in a gelling time of approximately 35 min. At approximately 10th min into the gelation process, 600 μL of the gelling solution was pipetted onto a mica sample plate on a spin coater (Chemat Technology Inc., Northridge, CA) with a speed of 3000 rpm and allowed to gel for 10 sec. The sample was then transferred from the spin coater to a sample holder where it is exposed to methanol vapor until the vesicle solution was deposited.

Bilayer Formation: DOPC, DSPC and 1-Palmitoyl-2-[6-[(7-nitro-2-1,3-benzoxadiazol-4-yl)amino]hexanoyl]-sn-Glycero-3-Phosphocholine (NBD-PC) were purchased from Avanti Polar Lipids (Alabaster, AL). 2:1 mole ratio of DOPC:DSPC and 1 mole % (of the fluid phase) of NBD-PC were mixed in a glass reaction vial and dried under a stream of nitrogen. Lipids were then resuspended in Nanopure water to 1 mg/ml total lipid concentration. The solution was held in a water bath at 65 ºC for 5 min. After heating, the solution was sonicated with a tip sonicator (Branson Sonifier, Model 250, Branson Ultrasonics, Danbury, CT) for a minute to obtain small unilamellar vesicles. The solution was then pipetted onto the xerogel and freshly cleaved mica surfaces to form a droplet for vesicle fusion. The supported lipid bilayer was placed in a temperature-controlled oven (Echotherm Chilling Incubator, Model IN35, Torrey Pines

Scientific, San Marcos, CA) at 65 ºC for 30 min. The system was then cooled to the room temperature with a cooling rate of 20 ºC/h. The lipid bilayers supported by xerogel and mica surfaces were placed in pure water at room temperature and excess vesicles were removed by rinsing.

The lipid bilayers and the xerogel surface were scanned with Digital Instruments Dimension 3100 Atomic Force Microscope (Santa Barbara, CA) equipped with Nanoscope software. Fluorescence imaging of bilayers and the FRAP experiments were carried out with Nikon Eclipse 400 Fluorescence Microscope (Nikon, Melville, NY) equipped with a fluorescence filter cube (EF-4 FITC HYQ, Nikon) which matches to the excitation and emission spectrum of NBD-PC. Images were captured with a CCD camera (Cascade II 512, Photometrics, Tucson, AZ) and the FRAP images were captured by an Orca digital camera (Hamamatsu, Japan) at varying periods of time after 10 s of photobleaching a spot with a diameter of 60 μm. The fluorescence recovery images were captured with the excitation light that was attenuated at least 400 times to prevent further bleaching. The fluorescence intensity with respect to time data was fitted to recovery curves by means of MatLab program. Fluorescence correlation spectroscopy (FCS) measurements were performed on a home-build FCS apparatus based on a Nikon TE2000 inverted fluorescence microscope by using Texas-Red DHPE as the fluorescent probe in the bilayer because of its high photostability. Experimental detail is described elsewhere.[13] In brief, a 568nm laser beam was coupled into the light path of the microscope by a dichroic mirror and focused by a 100X TIRF objective (Nikon Corp., Tokyo, Japan) onto the sample to excite the fluorescent probes. The FCS spot size was about 560 nm in diameter. The emission light was filtered by a 568 nm notch filter (Kaiser Optical Systems, Ann Arbor, MI) and a confocal pinhole (50 μm diameter, Thorlabs, Newton, NJ), then split by a 50/50 beam-splitter before finally

focused into two avalanche photo diodes (APD) (Perkin&Elmer, Canada). The photon arrival time is recorded and the cross-correlation between the two APD signals is calculated by a hardware correlator (correlator.com, Bridgewater, NJ) in real time. The correlation curves were then fitted to an analytical expression of normal 2-D diffusion using a nonlinear Levenberg-Marquardt algorithm.

Results and Discussion

Silica xerogel structure is highly dependent on the processing parameters such as reactant concentrations. The silica xerogel substrates used in this work were produced under the same experimental conditions, and their surface morphology was characterized by AFM (Figure 1) as the first step in this study. Cross sections of samples on four different sample sets were found to have an average feature size of 50 ± 21 nm (example features are circled in Figure 1.a and b). The average root mean-square (RMS) roughness value for the silica xerogel thin films obtained from 1 μm x 1 μm images was found to be 1.82 ± 0.19 nm.

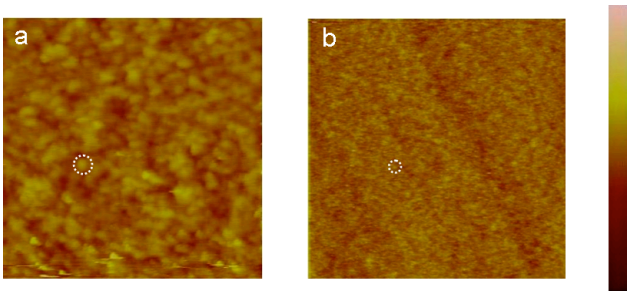

Figure 1. AFM image of silica xerogel surface (a) 1μm x1μm image (b) 20 μm x 20 μm image. The color scale bar represents 15 nm.

When the DOPC-DSPC vesicle solution was deposited on these surfaces, successful vesicle fusion and domain formation was observed (Figure 2.a and 2.b). In order to compare the surface topology of the lipid bilayer on rough surfaces to smooth surfaces, the same lipid solution was also deposited on mica (Figure 2.c) which is known to be atomically smooth. The surface of the lipid bilayer on silica xerogel is quite similar to the surface of the silica xerogel indicating that the bilayer follows the xerogel surface closely rather than being suspended on the substrate under contact mode AFM imaging conditions (Figure 2.a and Figure 1.b). The average RMS roughness values for xerogel and xerogel supported lipid bilayers obtained from 20 μm x 20 μm images were 0.71±0.28 nm and 0.59±0.04 nm, respectively, which are not significantly different from each other (t-test, $p \leq 0.05$). However, in contact mode imaging, there is a possibility that the tip would push the lipid bilayer towards the surface of the substrate and make it appear as if the bilayer is following the surface features. In order to reduce this effect, a certain spot on the sample was scanned in tapping mode (Figure 2.b) and then in contact mode AFM and the lipid bilayer was observed to be following the surface by both methods. As opposed to the xerogel supported bilayers, the mica supported bilayers were smoother having average RMS values of 0.07±0.01 nm (Figure 2.c).

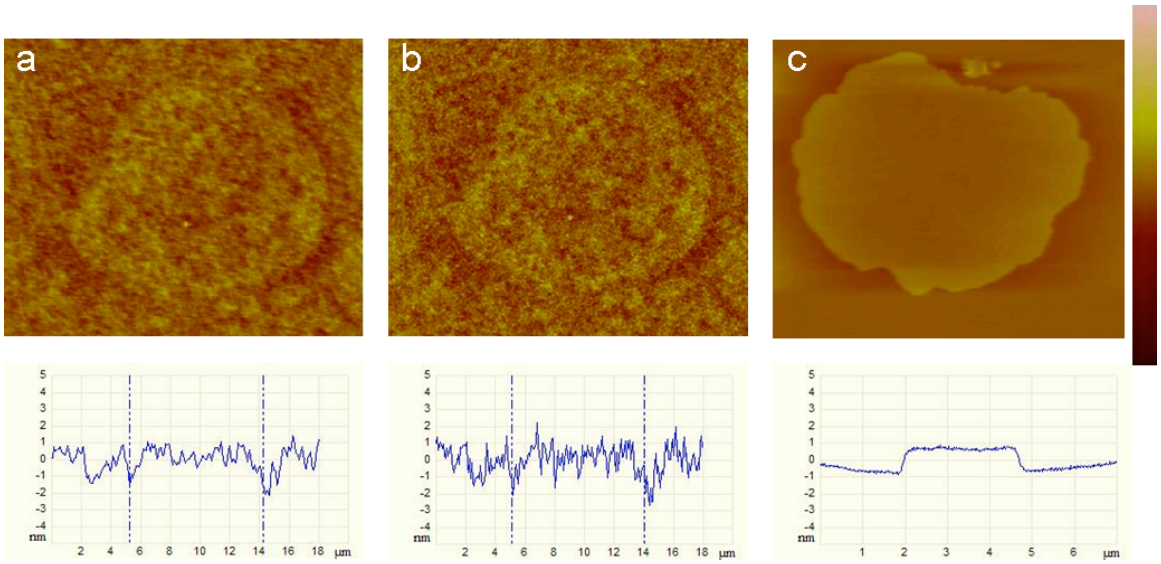

Figure 2. AFM images and line scans of DOPC-DSPC bilayer on (a) silica xerogel in contact mode, (b) silica xerogel in tapping mode, (c) on mica in contact mode. The dotted lines in the line scans for xerogel images indicate the edges of the DSPC domains. (a,b) 15.5 µm x 19 µm, (c) 8.3 µm x 9.5 µm. The color scale bar represents 15 nm.

If the actual bleached surface area is larger than the projected area, this gives rise to a smaller diffusion coefficient for rougher surfaces since the projected distance that a molecule travels decreases if the bilayer is following the surface roughness. For instance, Weng et al. (2004) observed that the diffusion coefficients of L-α-phosphatidylcholine (egg PC) on silica xerogel surfaces calculated by FRAP experiments (2±1 $\mu m^2/s$) was higher compared to the silica aerogels (0.6±0.2 $\mu m^2/s$) having higher roughness and smaller beads, therefore, they qualitatively concluded that the lipid bilayer follows the surface to some extent.[8] In our study, the lipid diffusion coefficient in pure DOPC on silica xerogels calculated by FRAP was 1.69±0.53 $\mu m^2/s$ which is consistent with the previous results. On the other hand, the lipid diffusion coefficient of

pure DOPC on mica was found to be significantly higher than on silica xerogels (3.93±0.98 $\mu m^2/s$). However, by analyzing the xerogel surface structures using AFM, the actual surface area was calculated to be only ~2% larger than the projected area (30 different images of 1μm x 1μm size). Such a low area change suggests that the surface roughness effect in terms of the distance that molecules travel on FRAP results could not be significant in this case. However, here, the AFM tip limitations become important. Continuous bilayers that penetrate into the deeper pores which cannot be detected by the AFM tip could be formed on highly porous silica xerogel increasing the real area for the FRAP calculations.

To account for the actual amount of lipid bilayer area compared to the projected area, we decided to compare the fluorescence intensity difference between the surrounding fluid phase and symmetrically distributed (spanning both leaflets) domains on mica vs. xerogel. The assumptions are that the domain intensity is attributed almost entirely to background and that fluorescence difference can be directly related to lipid density. All the domains on mica were symmetrically distributed (spanned both leaflets) as it is evident in the AFM image in Figure 2.a (hydrophobic mismatch is ~1.8 nm for symmetric DSPC domains in DOPC[14]). As for the silica xerogel, the AFM images are not sufficient to conclude whether the domains are symmetric or not because of the roughness of the xerogel surface. However, in Figure 3.a, we were fortunate to observe the presence of domains containing asymmetrically as well as symmetrically distributed domains on the xerogel (Figure 3, the intensity difference between the domain and the surroundings for line 1 (asymmetric domain) is approximately half of line 2 (symmetric domain)). In most of the other xerogel images, the domain intensities profiles resembled line 2 and were uniform allover the sample (Figure 3.b, the intensity profile of line 3 matches with line 2 rather than line 1). Thus, it was concluded that the domains on silica xerogel are mostly

symmetric. The intensity difference between 60 different symmetric domains and surrounding fluid phase were found to be 1.96±0.26 times higher for the bilayer supported on xerogel compared to 60 symmetric domains on mica. A plausible explanation for this result is that the bilayer penetrates into the pores and almost envelops half of the first layer of the silica beads on the surface. Modifying the area in the FRAP equations used for calculating the diffusion coefficient on silica xerogels accordingly resulted in a value of 3.31±1.05 $\mu m^2/s$ which is not statistically different from the diffusion coefficient on mica (3.93±0.98 $\mu m^2/s$). The agreement between diffusion coefficient and membrane area gives credence to the idea that there is significant coverage of the silica beads by the lipid bilayer.

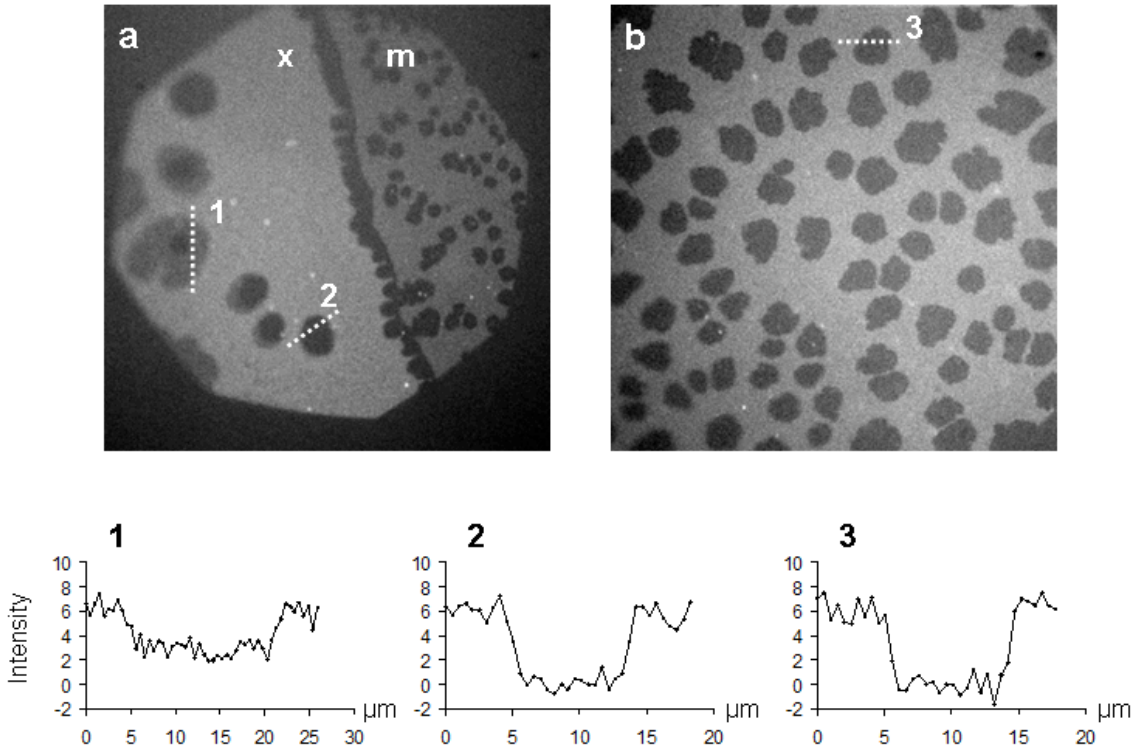

Figure 3. Fluorescence images of DOPC/DSPC bilayers (a) taken at xerogel/mica interface; x: xerogel part, m: mica part, (b) on silica xerogel. The bottom graphs are the scans of the dashed

lines indicated in the fluorescence images. The background intensity was set at the pixel intensity in the middle of the symmetric domains and subtracted out. The domain in image (b) corresponds to a symmetric domain as compared to the line scan of 2. The fluorescence images are both 130 μm x 130 μm.

The mica supported lipid bilayer in this study is free of defects at the scale of 200 nm that would be detectable as is evident from Fig. 2.c., whereas, it would be almost impossible to observe defects at that scale in silica xerogel supported bilayers by AFM due to the penetrating nature of the lipid bilayer. However, a recent study in the literature reported that the L-α-dimyristoyl phosphatidylcholine (DMPC) lipid bilayers can cover silica particles that are larger than 22 nm in diameter. On the contrary, if the particle size is between 1.2-22 nm, holes having the same diameter as the particles are formed around the silica particles due to the high curvature.[15] Since the silica bead size on the surface in our study is larger (50 ± 21 nm) than this range, the formation of continuous bilayers with minimal presence of defects may be expected. Another study published recently reported that the lateral diffusion coefficients of lipids on glass surfaces calculated by FRAP is lower than FCS results. This difference was attributed to the presence of defects in the lipid bilayer which are more pronounced in the larger FRAP spot compared to the FCS spot.[16] In our study, on the other hand, the FRAP and FCS results were very similar on both mica and silica xerogel (Table 1) supporting the argument that defect formation may be negligible and continuous bilayer formation could be achieved on both substrates.

Table 1. A comparison of the lipid bilayer properties on silica xerogel and mica. The values listed are in terms of means ± standard deviations. The results were compared by t-test ($p \leq 0.05$). The results for silica xerogel and mica were significantly different. There was no significant difference between the FRAP and FCS results.

	Silica Xerogel	**Mica**
Diffusion coefficient calculated by FRAP, $\mu m^2/s$	1.69±0.53	3.93±0.98
Diffusion coefficient calculated by FCS, $\mu m^2/s$	1.65±0.26	4.31±0.13
Number of domains / Area, $1/\mu m^2$	35.75×10^{-4}	35.59×10^{-4}
Domain size, μm^2	68.12±40.04	49.06±27.04
Domain area / Total area	0.224	0.176

Domain density and size on the silica xerogel surfaces were analyzed and compared to mica by using fluorescent images (Table 1). The data suggests that the number of domains per projected area is almost the same for both substrates, whereas the domains on silica xerogel are somewhat larger than on mica. Consequently, the domain area/projected area ratio is slightly higher for silica xerogel. However, if we assume the area increase factor of ~2 calculated above for both fluid and gel phases (since gel phase is stiffer than the fluid phase, the area increase factor would be less than 2 in the real case), the number of the domains per area on xerogel would decrease to half and the average domain area would increase to its twice value. However, the change in the domain area/total area ratio would not change. The difference between the domain area/total area ratios of silica xerogel and mica (0.224 vs. 0.176) possibly reflects a slight alteration of the liquidus and/or solidus curves of the binary phase diagram resulting in a change in gel/fluid ratio

at the same total composition of lipids. This means that the xerogel substrate changes the phase behavior of the lipid mixture only slightly, whereas it changes the nucleation behavior considerably. A possible reason for this behavior might be the presence of fixed nucleation sites in the silica xerogel substrates which is in accordance with our ongoing experiments.

Conclusions

Two phase lipid bilayers were formed on rough silica xerogel surfaces and compared to mica supported bilayers. The lipid bilayer was observed to be following the surface contours. The lateral diffusion coefficient of the lipids on silica xerogel was found to be lower than on mica mainly due to the bilayer following the substrate roughness. The domains formed on silica xerogel were observed to be symmetric but of lower density than the domains on mica. These results indicate that a continuous multi-phase lipid bilayer can be prepared on a nanoporous xerogel surface. Future work will focus on increasing bilayer stiffness by using higher amounts of gel phase lipids to decrease bilayer corrugation and addition of cholesterol and inclusion of transmembrane proteins in this xerogel supported lipid bilayer system.

Acknowledgements

We acknowledge funding by the NSF NIRT Program (CBET 0506602) and the NSF MRSEC Program CPIMA (NSF DMR 0213618). This work was performed under the auspices of the U.S. Department of Energy by Lawrence Livermore National Laboratory in part under Contract W-7405-Eng-48 and in part under Contract DE-AC52-07NA27344.

References

(1) Bayerl, T. M.; Bloom, M. *Biophys. J.* **1990,** 58, 357-362.

(2) Fromherz, P.; Kiessling, V.; Kottig, K.; Zeck, G. *Appl. Phys. A* **1999,** 69, 571-576.

(3) Salafsky, J.; Groves J. T.; Boxer, S. G. *Biochemistry* **1996,** 35, 14773-14781.

(4) Drexler, J.; Steinem, C. *J. Phys. Chem. B* **2003,** 107, 11245-11254.

(5) Römer, W.; Steinem, C. *Biophys. J.* **2004,** 86, 955-965.

(6) Wattraint, O.; Arnold, A.; Auger, M.; Bourdillon, C.; Sarazin, C. *Anal. Chem.* **2005,** 336, 253-261.

(7) Doshi, D. A.; Dattelbaum, A. M.; Watkins, E. B.; Brinker, C. J.; Swanson, B. I.; Shreve, A. P.; Parikh, A. N.; Majewski, J. *Langmuir* **2005,** 21, 2865-2870.

(8) Weng, K. C.; Stålgren, J. J. R.; Duval, D. J.; Risbud, S. H.; Frank, C. W. *Langmuir* **2004,** 20, 7232-7239.

(9) Weng, K. C.; Stålgren, J. J. R.; Risbud, S. H.; Frank, C. W. *J. Non-Cryst. Solids* **2004,** 350, 46-53.

(10) Helms, J. B.; Zurzolo, C. *Traffic* **2004,** 5, 247-254.

(11) Keller, P.; Toomre, D.; Diaz, E.; White, J.; Simons, K. *Nat. Cell Bio.* **2001,** 3, 140-149.

(12) Devaux, P. F. *Biochemistry* **1991,** 30, 1163-1173.

(13) Forstner, M. B.; Yee, C. K.; Parikh, A. N.; Groves, J. T. *J. Am. Chem. Soc.* **2006,** 128, 15221-15227.

(14) Blanchette, C. D.; Lin, W. C.; Orme, C. A.; Ratto, T. V.; Longo, M. L. *Langmuir* **2007,** 23, 5875-5877.

(15) Roiter, Y.; Ornatska, M.; Rammohan, A. R.; Balakrishnan, J.; Heine, D. R.; Minko, S. *Nano Lett.* **2008,** 8, 941-944.

(16) Guo, L.; Har, J. Y.; Sankaran, J.; Hong, Y. M.; Kannan, B.; Wohland, T. *ChemPhysChem* **2008,** 9, 721-728.

TOC Graphic